metals

MDPI

Article

On the Step Cooling Treatment for the Assessment of Temper Embrittlement Susceptibility of Heavy Forgings in Superclean Steels

Roberto Roberti and Michela Faccoli *

Department of Mechanical and Industrial Engineering, University of Brescia, Via Branze, 38, Brescia 25123, Italy; rroberti.bs@gmail.com

* Correspondence: michela.faccoli@unibs.it; Tel.: +39-030-3715572

Academic Editor: Hugo F. Lopez

Received: 20 July 2016; Accepted: 29 September 2016; Published: 10 October 2016

Abstract: When subjected to extended exposure to intermediate service temperatures, Cr–Mo steels, Ni–Cr steels, and 5% Ni steels can become embrittled, with an associated decrease in fracture toughness and a shift in the ductile-to-brittle transition temperature to higher temperatures. Two methods for the investigation of temper embrittlement phenomena are isothermal aging or the use of a step cooling aging treatment, which is less time consuming and is considered to be the most severe test to evaluate steel's susceptibility to this phenomenon. In the present work, the effectiveness of the step cooling treatment in the assessment of temper embrittlement in a superclean 26NiCrMoV14.5 steel for heavy section forgings has been studied. Some isothermal aging treatments in the critical temperature range have also been carried out. Results of a Charpy V impact test on not-aged and aged specimens, and observation of the fracture surfaces led to the following conclusions: the steel does not undergo temper embrittlement upon step cooling treatment or after aging at different temperatures and times in the critical temperature range; the most negative effect on the shift of the ductile-to-brittle transition curve—compared with not aged steel—has been observed after aging at 593 °C for 2 h (ΔT54J = 9 °C); further aging up to 8 h produced a ΔT54J of only 1 °C. Neither step cooling nor aging at various critical temperatures gave rise to an intergranular brittle fracture; the amount of embrittling impurity elements in a superclean steel does not seem to be enough to cause embrittlement and a pure intergranular decohesion.

Keywords: temper embrittlement; step cooling; superclean steels; heavy forgings; Charpy impact tests; fracture mechanisms

1. Introduction

For a long time, many research works have reported the influence of grain boundary segregation of either impurities or alloying elements on the temper embrittlement of Cr–Mo steels [1–3], Ni–Cr steels [4,5], and 5% Ni steels [6].

When subjected to extended exposure to intermediate service temperatures, these steels can become embrittled with an associated decrease in fracture toughness and a shift in ductile-to-brittle transition temperature (DBTT) to higher temperatures. The embrittlement—which is referred to as temper embrittlement—is mainly caused by changes in the microchemistry of grain boundaries, which becomes the preferred path for fracture [7–16]. Temper embrittlement is a not-hardening embrittlement and stems from grain boundary segregation of impurity elements as a result of prolonged exposure in the temperature range of 350–600 °C.

However, it must be underlined that two embrittlement mechanisms superimpose for these types of alloys during aging in the embrittlement temperature range, namely: (a) the gradual migration

of impurity elements such as P, Sn, As, and Sb to prior austenite grain boundaries, which results in the so-called reverse temper embrittlement [17–19] and (b) changes in the size and morphology of carbides for long aging times, which also cause brittleness of the steels [20,21]. Both impurity migration and carbide modification are known to be temperature-activated phenomena. However, different temperatures do not necessarily result in the same microstructural and embrittling effect: the migration rate of impurities may vary from element to element, while high temperature may also produce a redistribution of impurity elements (reverse embrittlement), and equilibrium size and morphology of carbides are influenced by the level of temper temperature.

Factors affecting temper embrittlement are suggested to be chemical composition, temperature, holding time, and applied stress [18,22]. Among these factors, the effect of chemical composition and temperature on temper embrittlement has been thoroughly investigated by most studies. For example, it is universally agreed that when the amount of impurities increases, the steel is more prone to temper embrittlement. Moreover, considering that the diffusion rate strongly depends on both time and temperature, one should be also aware of the effect of time and temperature. The higher the temperature and the longer the time of diffusion, the more the amount of segregated embrittling elements should be; hence, the greater the embrittlement effect should be on the alloy.

Two methods for the investigation of temper embrittlement phenomena are isothermal aging (holding the alloy for a long time at a constant temperature) or the use of a step cooling aging treatment. Step cooling aging was introduced principally to study the effect of cooling from post-weld heat treatment (PWHT) in large components, whose cooling rate is long enough to induce embrittlement in particular in not superclean steels. For superclean steels, it is also of interest to study the effect of working conditions on embrittlement. Since isothermal aging at low temperatures requires a long period of time, it is a time-consuming method; the step cooling aging treatment for embrittlement investigations can therefore be considered for this purpose.

Figure 1 shows a typical step cooling operation which is in use by the American Petroleum Institute (API) [23]; low heating and cooling rates are as well specified (as reported below), and their contribution to damage accumulation is as important as holding at constant temperature. This treatment consists of: heating to 316 °C (heating rate not critical); heating at 56 °C/h to 593 °C; holding at 593 °C for 1 h; cooling at 6 °C/h to 538 °C; holding at 538 °C for 15 h; cooling at 6 °C/h to 524 °C; holding at 524 °C for 24 h; cooling at 6 °C/h to 496 °C; holding at 496 °C for 60 h; cooling at 3 °C/h to 468 °C; holding at 468 °C for 100 h; cooling at 28 °C/h to 315 °C; and cooling to room temperature in still air.

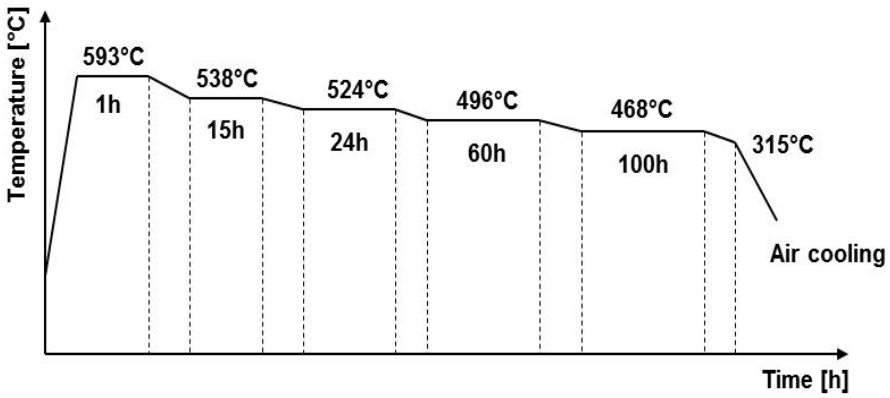

Figure 1. Step cooling heat treatment carried out on the investigated superclean steel.

To assess the amount of temper embrittlement, the fracture appearance transition temperature (FATT) and the 54 J (40 ft-lb) transition temperature (TT54J)—as standardized for petrochemical reactors [23], before and after aging or step cooling treatment—are usually measured. The temper embrittlement manifests itself as an increase in these parameters [24].

A different way of assessing the sensitivity of steels to temper embrittlement is represented by the *J*-Factor, defined by Watanabe et al. [25]:

$$J\text{-Factor} = (\text{Mn} + \text{Si}) \cdot (\text{P} + \text{Sn}) \cdot 10^4 \quad (1)$$

The *J*-Factor is a dimensionless factor related to the amount of indicated elements in wt %, and its value is used as a measure of the sensitivity of steel to temper embrittlement. For low alloy Cr–Mo steels, a limit of 100 has usually been set for its value; with the introduction of secondary metallurgy technologies for clean and ultra clean steels, lower and lower limits have been continuously proposed for the *J*-Factor.

In the last decades, many studies have been carried out [21,26–28] aiming at a complete understanding of temper embrittlement, and different interesting theories have been proposed to explain the various factors that influence it. A recent interpretation of the phenomenon is based on the concept of non-equilibrium grain boundary segregation of impurity elements, particularly phosphorus [29–31]. According to this theory, the embrittlement increases in the first period of aging of the steel; as a consequence, the transition temperature (FATT) increases, and an intergranular fracture mechanism is observed. This embrittlement is due to impurity elements in the steel—in particular, phosphorus—that migrate to prior austenite grain boundaries and concentrate in solid solution close to them. For longer aging times, a decrease of embrittlement is then observed, and this effect is explained by the fact that the initial segregation of impurity elements is a non-equilibrium segregation. Therefore, after the initial segregation, the grain boundary concentration of phosphorus is much higher than in the grain interior, and the reverse diffusion of phosphorus towards grain interior prevails. Then, desegregation of phosphorus continues until it disappears after a certain period of time, when the diffusion process reaches full equilibrium [31].

The role of the alloying elements towards temper embrittlement is not less important than that of impurity elements. The presence of Ni, Cr, Mn, and Mo in the steel remarkably increases the segregation, as they co-segregate with impurities; however, these elements segregate to grain boundaries only in steels containing impurity elements [12].

Impurity elements (and some alloying elements) have a strong interaction that facilitates the reciprocal segregation; an impurity atom attracts atoms of an alloying element more easily than iron atoms, so the co-segregation of "impurity–alloying element" is highly favored. For example, this is the behavior of the couples P and Ni, P and Cr, and Sb and Cr. Furthermore, the presence of more than one alloying element is more effective in promoting the segregation of an impurity element to grain boundaries.

In the present work, the effectiveness of the step cooling treatment in the assessment of temper embrittlement in a superclean steel for heavy section forgings has been studied; up to now, the step cooling treatment is indeed considered to be the most severe test to evaluate steel's susceptibility to this phenomenon. In addition to the complete step cooling treatment, some isothermal aging treatments have been carried out in the critical temperature range of temper embrittlement to investigate their effect on embrittlement.

Afterwards, fractographic observations of the broken specimens have been carried out by means of scanning electron microscopy (SEM) to thoroughly investigate the fracture mechanisms at various temperature test conditions.

2. Materials and Methods

The steel investigated in the present paper is a 26NiCrMoV14.5 superclean steel, characterized by the chemical composition shown in Table 1.

Table 1. Chemical composition in weight percent of the investigated superclean steel.

C	Mn	Si	P	S	Cu	Cr	Ni	Mo	Sn	Al	V	Nb	Ti	B	As	Sb	Co
0.26	0.04	0.02	0.003	0.001	0.03	1.66	3.62	0.40	0.004	0.004	0.087	0.003	0.002	0.0002	0.0004	0.0004	0.006

This steel has been fabricated by ASO Siderurgica S.r.l. (Ospitaletto, Italy), starting from a selected scrap charge and according to a specially developed operative practice through an Linz-Donawitz furnace and vacuum degassing secondary metallurgy. The steel is used for a heavy section forged ring to be employed in the power generation industry.

The *J*-Factor for the produced superclean steel is calculated by putting the weight percents of Mn, Si, P, and Sn in Equation (2). The obtained value is well below the limit given for normally clean steels, which is around one order of magnitude greater [32].

$$J\text{-Factor} = (0.02 + 0.04) \times (0.003 + 0.004) \times 10^4 = 4.2 \quad (2)$$

A number of steel blocks (130 × 130 × 210 mm) have been machined out from the forged and heat-treated ring, and have been aged as follows at various temperatures in the critical range for temper embrittlement. First of all, the step cooling heat treatment shown in Figure 1 has been carried out as the reference embrittlement aging. The other aging treatments have been carried out at constant temperature, and each of them is a multiple of one single step of the step cooling treatment. The aging treatments carried out on the investigated superclean steel are reported in Table 2.

Table 2. The investigated steel's aging conditions.

Steel Condition	Temperature (°C)	Time (h)
A	524	120
B	593	2
C	538	48
D	not aged material	
E	step cooling (Figure 1)	
F	593	8

Charpy impact test specimens have been machined out from each as received (not aged) or aged steel block. The impact tests have been carried out using a Wolpert Probat PW 30/15 Charpy pendulum, in the range from −196 °C to room temperature, complying with ASTM E23.

Fractographic observations of broken specimens have been carried out by means of a scanning electron microscope LEO EVO 40XVP with microprobe Link Analytical eXL.

3. Results and Discussion

Charpy-V impact test ductile-to-brittle transition curves have been obtained both for the not aged material and for all aging treatment conditions, as shown in Figure 2.

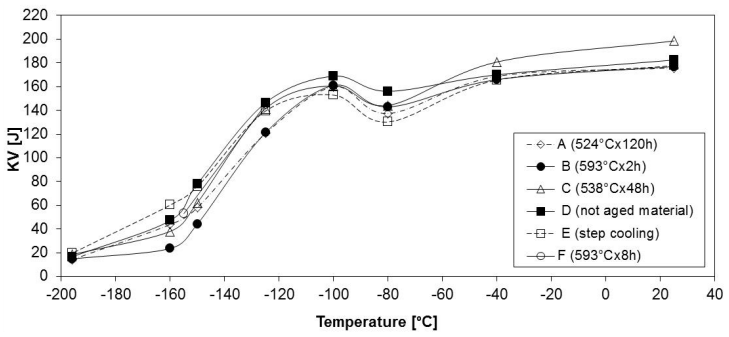

Figure 2. Ductile-brittle transition fracture curves.

From Figure 2, it can be observed that for all aging treatments carried out from 524 °C to 593 °C, (except the one at 593 °C for 8 h), there is a shift of the transition curves to higher temperatures compared with the curve of the not-aged steel. Many of the curves, however, intersect each other, and therefore the degree of shift towards higher temperatures depends on the level of impact energy.

It is also evident that the ductile-brittle transition fracture curve for the step cooling treatment and for other aging treatments show differences either in some impact value levels or in the shift of the ductile-to-brittle transition, because most probably the various aging temperatures not only have a different influence on the diffusion of impurity and alloying elements which play a role in the temper embrittlement process, but also have a different effect on the modification of carbides which influences the transition from ductile-to-brittle (cleavage or quasi-cleavage) fracture, and may enhance the scatter of the fracture behavior.

In particular, Figure 2 shows that the aging treatment B (593 °C × 2 h) seems to have the most negative effect (ΔT54J = 9 °C) on the shift of the ductile-to-brittle transition curve. On the contrary, aging at the same temperature for 8 h (aging treatment F) induces a less negative effect (ΔT54J = 1 °C). It could be then concluded that at 593 °C the migration of embrittling elements does not occur, and progressive modification of carbides at increasing treatment time results in an improvement of the fracture behavior.

The longest aging treatment (aging treatment A, 524 °C × 120 h) shifts the curve to higher temperatures (ΔT54J = 2.5 °C) than the step cooling treatment (ΔT54J = −9 °C); indeed, the step cooling treatment apparently induces an improvement in the fracture behavior (negative shift of the ΔT54J), but this is most probably due to the scatter of impact toughness and its effect on drawing the transition curve.

Figure 3 shows the ductile-brittle transition fracture curves for the not aged steel and after the step cooling treatment for the steel investigated in this work, compared with the corresponding curves obtained by Bourrat and Schaff [33] for an 11% CrNiMoV superclean steel.

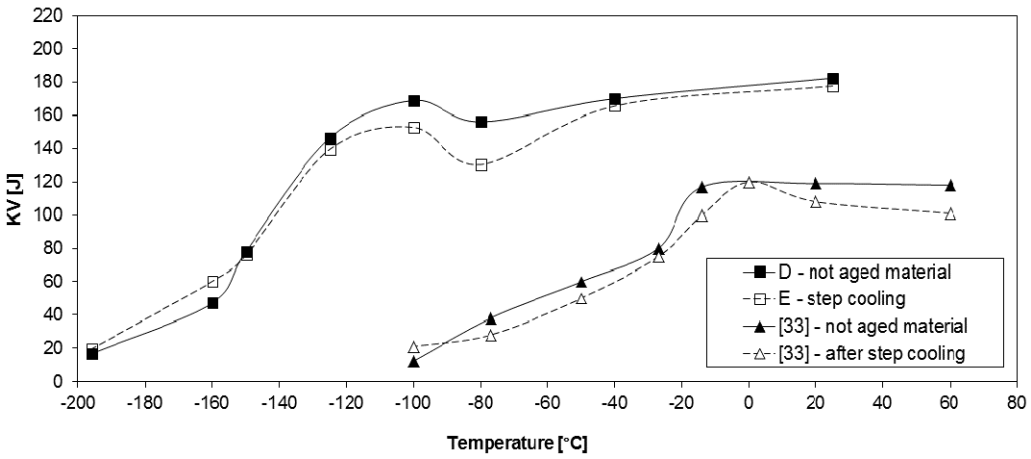

Figure 3. Impact test ductile-to-brittle transition curves for not aged and after step cooling conditions for the investigated steel and for a 11% CrNiMoV heat resistant superclean steel [33].

From Figure 3, it is evident that for both the superclean steels, the ductile-to-brittle transition curves for the not aged steel and after the step cooling treatment are very close each other, although for the 11% CrNiMoV steel, a ΔT54J of about 12 °C is observed, notwithstanding its very low *J*-Factor = 1.8 (P = 0.0025%, As = 44 ppm, Sb = 3 ppm, Sn = 13 ppm). These results confirm the low susceptibility of superclean steels to temper embrittlement and suggest that the eventual shift of the impact transition curve is to be related to a fracture mechanism different from intergranular fracture, which enhances the impact toughness scatter.

From the examination of the fracture surface of broken specimens, it could be concluded that none of the tested specimens failed—even partially—by intergranular fracture (i.e., the typical fracture mechanism of temper embrittled microstructures). For this reason, it is not possible to associate any of the ΔT54J shift in the ductile-to-brittle transition curves to a temper embrittlement mechanism. Most probably, the amount of atoms of impurity elements available for diffusion towards grain boundaries is not enough to cause embrittlement and a pure intergranular decohesion.

The observed transition of fracture at decreasing temperature goes from a ductile rupture to an almost complete transgranular quasi-cleavage mechanism with only some quasi-cleavage grain facet (as shown in Figures 4–6).

In the test temperature range −196 °C to −150 °C, all of the impact specimens presented an analogous quasi-cleavage fracture mechanism (see Figure 4 as an example), except for the not aged specimens, for which no quasi-cleavage grain facets were observed.

In the test temperature range −150 °C to −80 °C, the observed fracture surfaces presented a mixed ductile-brittle fracture for all not aged and aged specimens. Figure 5 is representative of this fracture.

In the test temperature range −80 °C to room temperature, the observed fracture surfaces presented a fully ductile fracture for all not aged and aged specimens. Figure 6 is representative of this fracture appearance and shows the ductile fracture of the sample subjected to step cooling treatment and tested at −40 °C.

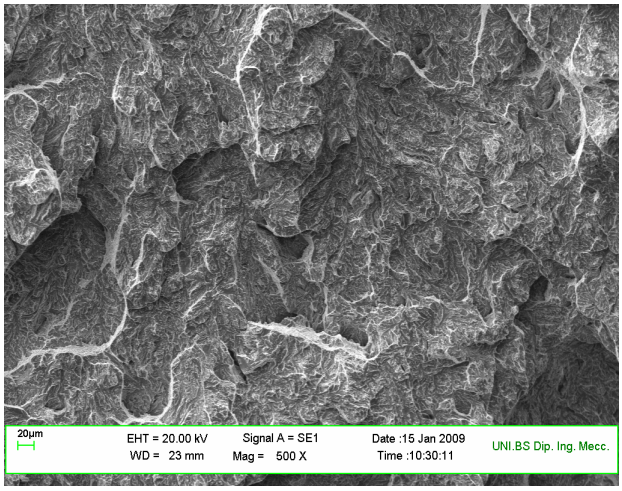

Figure 4. Fracture surface of the sample aged at 593 °C for 8 h, tested at −150 °C.

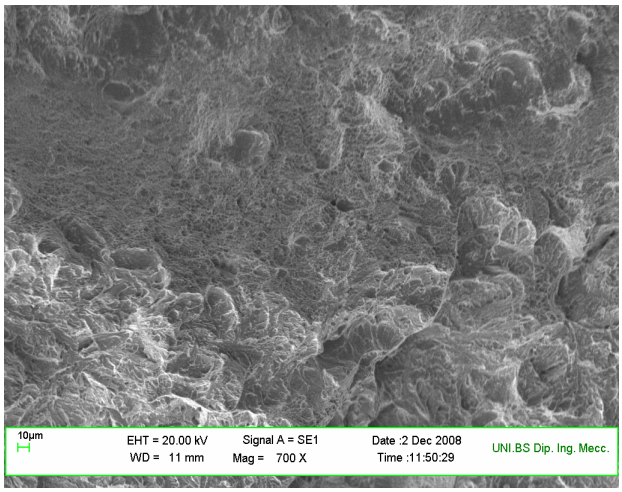

Figure 5. Fracture surface of the sample aged at 524 °C for 120 h and tested at −80 °C.

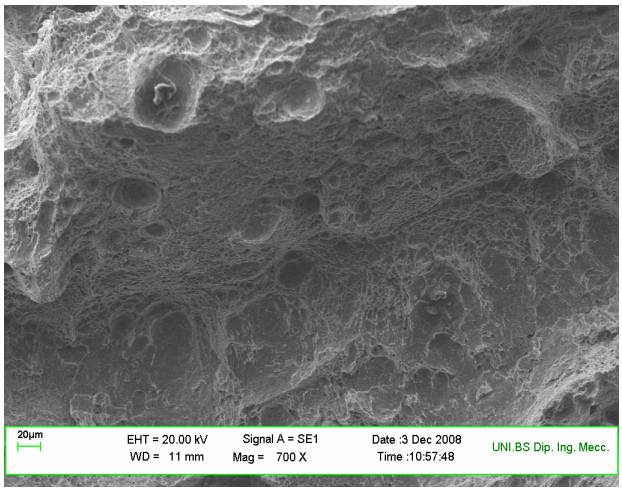

Figure 6. Fracture surface of the sample subjected to step cooling treatment and tested at −40 °C.

4. Conclusions

The temper embrittlement of a 26NiCrMoV14.5 superclean steel has been studied by aging it either according to the API step cooling treatment or by aging at constant temperature. In the latter case, aging temperature corresponded to one of the step cooling temperatures, while aging time was a multiple of the same step time.

Results of Charpy V impact test on not aged and aged specimens and observation of the fracture surfaces led to the following conclusions:

(a) Superclean 26NiCrMoV14.5 steel does not undergo temper embrittlement upon step cooling treatment or after aging at different temperatures and times in the critical temperature range. The maximum ΔT54J shift in the ductile-to-brittle transition curve—compared with not aged steel—has been observed after aging at 593 °C for 2 h (ΔT54J = 9 °C); further aging up to 8 h produced a ΔT54J of only 1 °C;

(b) Neither step cooling nor aging at various critical temperatures gave rise to an intergranular brittle fracture; the amount of embrittling impurity elements in a superclean steel does not seem to be enough to cause either temper embrittlement and/or a pure intergranular decohesion;

(c) Differences in the ductile-brittle transition curves as a function of the different aging treatments seem to be most probably related to the effect of additional tempering on the steel microstructure, and in particular to the modification of carbides, which influences the transition from ductile-to-brittle (cleavage or quasi-cleavage) fracture.

Acknowledgments: The authors wish to thank G. Straffelini and L. Maines, University of Trento, for their helpful contribution to the Charpy tests. The work is based on the degree thesis of the student S. Conforti, whose contribution is kindly appreciated.

Author Contributions: Roberto Roberti and Michela Faccoli conceived, designed and performed the experiments, they analyzed the data and wrote the paper.

Conflicts of Interest: The authors declare no conflict of interest.

References

1. Bruscato, R. Temper embrittlement and creep embrittlement in 2-1/4 Cr-1 Mo shielded metal arc weld deposits. *Weld. J. Res. Suppl.* **1970**, *49*, 148s–156s.
2. Wada, T. *Report RP-32-74-03*; Climax Molybdenum Company of Michigan: Detroit, MI, USA, 1975.
3. King, B.L.; Wigmore, G. Temper embrittlement in a 3-pct Cr-Mo turbine disc steel. *Metall. Trans. A* **1976**, *7*, 1761–1767. [CrossRef]

4. Briant, C.L.; Banerji, S.K. Tempered martensite embrittlement in phosphorus doped steels. *Metall. Trans. A* **1979**, *10*, 1729–1737.
5. Kameda, J.; McMahon, C.J., Jr. The effects of Sb, Sn, and P on the strength of grain boundaries in a Ni-Cr Steel. *Metall. Trans. A* **1981**, *12*, 31–37. [CrossRef]
6. A Study of Temper Embrittlement during Stress Relieving of 5Ni-CrMo-V Steels. Available online: http://www.astm.org/DIGITAL_LIBRARY/STP/PAGES/STP46473S.htm (accessed on 8 October 2016).
7. Temper Embrittlement of Rotor Steels. Available online: http://www.astm.org/DIGITAL_LIBRARY/STP/PAGES/STP46478S.htm (accessed on 8 October 2016).
8. Temper Brittleness—An Interpretive Review. Available online: http://www.astm.org/DIGITAL_LIBRARY/STP/PAGES/STP46479S.htm (accessed on 8 October 2016).
9. Mulford, R.A.; McMahon, C.J., Jr.; Pope, D.P.; Feng, H.C. Temper embrittlement of Ni-Cr Steels by phosphorus. *Metall. Trans. A* **1976**, *7*, 1183–1195. [CrossRef]
10. Briant, C.L.; Banerji, S.K. Intergranularfailure in steel: The role of grain-boundary composition. *Int. Met. Rev.* **1978**, *23*, 164–199. [CrossRef]
11. Lea, C.; Seah, M.P. Site competition in surface segregation. *Surf. Sci.* **1975**, *53*, 272–285. [CrossRef]
12. Guttmann, M.; Dumiulin, P.; Wayman, M. The thermodynamics of interactive co-segregation of phosphorus and alloying elements in iron and temper-brittle steels. *Metall. Trans. A* **1982**, *13*, 1693–1711. [CrossRef]
13. Erhart, H.; Grabke, H.J. Equilibrium segregation of phosphorus at grain boundaries of Fe–P, Fe–C–P, Fe–Cr–P, and Fe–Cr–C–P alloys. *Met. Sci.* **1981**, *15*, 401–408. [CrossRef]
14. Yuan, Z.X.; Song, S.H.; Faulkner, R.G.; Xu, T.D. Effect of cerium on temper embrittlement of P-doped Mn structural-steels. *Acta Metall. Mater.* **1994**, *42*, 127–132.
15. Pilkington, R.; Dicken, R.; Peura, P.; Lorimer, G.W.; Allen, G.C.; Holt, M.; Younes, C.M. Trace element embrittlement in a 2.25%Cr-1%Mo steel. *Mater. Sci. Eng. A* **1996**, *212*, 191–205. [CrossRef]
16. Phythian, W.J.; English, C.A. Microstructural evolution in reactor pressure vessel steels. *J. Nucl. Mater.* **1993**, *205*, 162–177. [CrossRef]
17. Wada, T.; Hagel, W.C. Effect of trace elements, molybdenum, and intercritical heat treatment on temper embrittlement of 2-1/4Cr-1 Mo steel. *Metall. Mater. Trans. A* **1976**, *7*, 1419–1426. [CrossRef]
18. Low, J.R., Jr.; Stein, D.F.; Turkalo, A.M.; Laforce, R.P. Alloy and impurity effects on temper brittleness of steel. *Trans. Metall. Soc.* **1968**, *242*, 14.
19. Yu, J.; McMahon, C.J. The effects of composition and carbide precipitation on temper embrittlement of 2.25 Cr-1 Mo steel: Part I. Effects of P and Sn. *Metall. Trans. A* **1980**, *11*, 277–289. [CrossRef]
20. Wignarajah, S.; Masumoto, I.; Hara, T. Evaluation and simulation of the microstructural changes and embrittlement in 21/4Cr-1Mo steel due to long term service. *ISIJ Int.* **1990**, *30*, 58–63. [CrossRef]
21. Seah, M.P. Grain boundary segregation and the T–t dependence of temper brittleness. *Acta Mater.* **1977**, *25*, 345–357. [CrossRef]
22. Suzuki, M.; Fukaya, K.; Oku, T. Effect of applied stress on temper embrittlement of $2_{1/4}$Cr-1Mo steel. *Trans. Iron Steel Inst. Jpn.* **1982**, *22*, 862–868. [CrossRef]
23. API Publication Standard No. 959. 1982. Available online: https://www.scribd.com/document/292425595/API-Publ-959 (accessed on 8 October 2016).
24. Buscemi, C.D.; Jack, B.I.; Erwin, N.E. Temper embrittlement in 2-1/4 Cr-1 Mo steels after 75,000-hour isothermal aging. *J. Eng. Mater. Technol.* **1991**, *113*, 329–335. [CrossRef]
25. Watanabe, J.; Shindo, Y.; Murakami, Y.; Adachi, T.; Ajiki, S. Temper embrittlement of $2_{1/4}$ Cr-1Mo pressure vessel steel. In Proceedings of the ASME 29th Petroleum Mechanical Engineering Conference, Dallas, TX, USA, 15–18 September 1974.
26. McMahon, C.J., Jr. Temper Embrittlement of Steels: Remaining Issues. *Mater. Sci. Forum* **1989**, *46*, 61–76. [CrossRef]
27. Hickey, J.J.; Bulloch, J.H. The role of reverse temper embrittlement on some low and high temperature crack extension processes in low carbon, low alloy steels: A review. *Int. J. Press. Vess. Pip.* **1992**, *49*, 339–386. [CrossRef]
28. Mclean, D. *Grain Boundaries in Metals*; Oxford University Press: London, UK, 1957; p. 118.
29. Sevc, P.; Anovex, J.J.; Lucas, M.; Grabke, H.J. Kinetics of phosphorus segregation in 2.7Cr-0.7Mo-0.3V steels with different phosphorus contents. *Steel Res.* **1995**, *66*, 537–542.

30. Zhang, Z.; Xu, T.; Lin, Q.; Yu, Z. A new interpretation of temper embrittlement dynamics by non-equilibrium segregation of phosphor in steels. *J. Mater. Sci.* **2001**, *36*, 2055–2059.
31. Li, Q.; Li, L.; Liu, E.; Liu, D.; Cui, X. Temper embrittlement dynamics induced by non-equilibrium segregation of phosphorus in steel 12Cr1MoV. *Scr. Mater.* **2005**, *53*, 309–313. [CrossRef]
32. Tanaka, Y.; Azuma, T.; Yaegashi, N. Isothermal aging test results up to 100,000 h of NiCrMoV steels for low pressure steam turbine. In *Materials Ageing and Component Life Extension*, Proceedings of the International Symposium on Materials Ageing and Component Life Extension, Milan, Italy, 10–13 October 1995.
33. Bourrat, J.; Shaff, H. Pitting and stress corrosion cracking of conventional and high purity LP turbine rotor steel. In Proceedings of the Clean Steel, Superclean Steel, London, UK, 6–7 March 1995; p. 157.